Title

ULTRASOUND IMAGING AND IDENTIFICATION OF MICROCALCIFICATION CLUSTERS BY CORRELATION OF SCATTER FROM MULTIPLE ANGLES

Author

Perez-Mendez, V.

Publication Date

1983-08-01

Lawrence Berkeley Laboratory
UNIVERSITY OF CALIFORNIA

Physics, Computer Science & Mathematics Division

Submitted to Ultrasound in Medicine and Biology

ULTRASOUND IMAGING AND IDENTIFICATION OF MICROCALCIFICATION CLUSTERS BY CORRELATION OF SCATTER FROM MULTIPLE ANGLES

V. Perez-Mendez, P. Wiedenbeck, P. Davis,
and C.J. Tzeng

August 1983

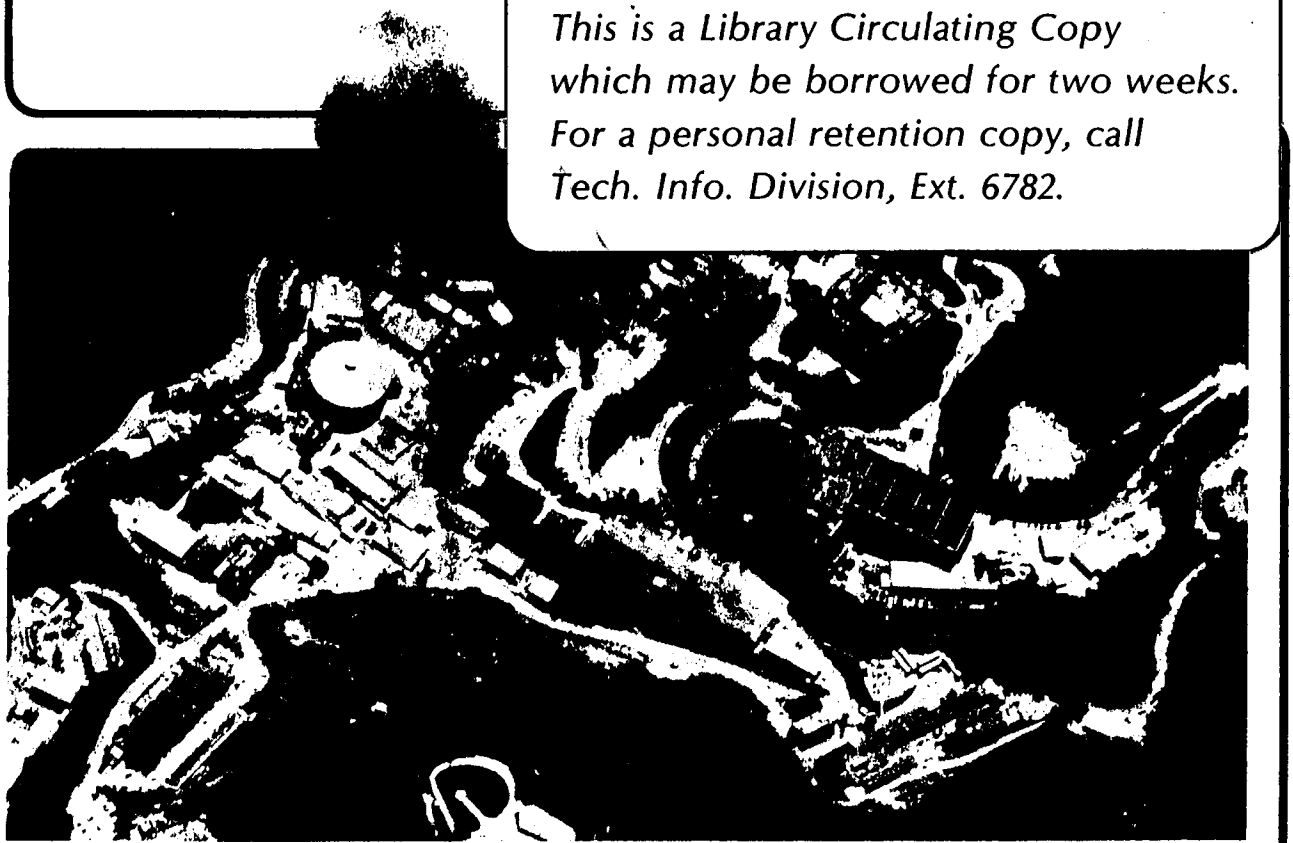

Prepared for the U.S. Department of Energy under Contract DE-AC03-76SF00098

DISCLAIMER

LBL-15939

ULTRASOUND IMAGING AND IDENTIFICATION OF MICROCALCIFICATION CLUSTERS BY CORRELATION OF SCATTER FROM MULTIPLE ANGLES

V. Perez-Mendez, P. Wiedenbeck, P. Davis and C.J. Tzeng

Radiology Department
University of California
San Francisco, California 94143
and
Lawrence Berkeley Laboratory
University of California
Berkeley, California 94720

August 1983

This work was supported by the U.S. Department of Energy under Contract No. DE-AC03-76SF00098.

ULTRASOUND IMAGING AND IDENTIFICATION OF MICROCALCIFICATION CLUSTERS BY CORRELATION OF SCATTER FROM MULTIPLE ANGLES

V. Perez-Mendez, P. Wiedenbeck, P. Davis and C.J. Tzeng
Radiology Dept. University of California, San Francisco, CA 94143
and
Laurence Berkeley Lab, Berkeley, CA 94720

ABSTRACT

Various types of malignant and benign breast tumors are associated with clusters of calcifications with grain sizes 0.1 to a few mm spread out over volumes of a few cc. A series of phantoms containing calcium carbonate grains embedded in a gelatin mixture were made and the ultrasound scattering patterns were measured with 2.25 MHz transducers. Scattering from the calcifications were distinguished from the larger reflections from tissue interfaces by computer correlation of the signals obtained from transducers placed at three different angles. An automatic gain control detection system was developed for the purpose of amplifying the signal to the right level for the computer correlation and to compensate for the attenuation of the ultrasound in the tissue.

INTRODUCTION

Various types of malignant and benign breast tumors are associated with clusters of calcifications with grain sizes ranging from 0.1 to 1 mm or larger (Murphy and DeSchryver-Kecskemti 1978). These clusters may contain as few as 5 or 6 grains or, in some cases, many tens of grains. The clusters may vary from spherical distributions of about 1 cm in diameter to elongated distributions spread out over several centimeters. The correlation between the existence of microcalcification clusters and some forms of carcinoma is believed to be greater than 80%.

Up to 45% of non-palpable breast cancers are only detected on x-ray

mammograms as a cluster of small calcifications (Wolfe 1974, Malone et al. 1975, Feig et al. 1977). Figure 1 shows an x-ray photograph of a typical microcalcification cluster. Since the patient receives radiation during mammography, it is useful to consider non-ionizing techniques such as ultrasound to determine whether these calcifications could be detected and their spatial distributions mapped out. It is assumed that the ultrasonic approach does not contribute any known hazard to the patient and could be used as a routine screening process. However, present commercially available ultrasound machines do not appear able to detect reliably most calcifications smaller than 5 mm in diameter (Sickles 1983).

We have shown previously that ultrasonic echoes from clusters of grains ranging in size from 0.1 to 1 mm and larger could be detected adequately above the background reflections from normal tissue (Perez-Mendez et al. 1979). In Figure 2, we show that for grains smaller than 0.3 mm in size, ultrasound frequencies of 2.25 to 5 MHz could be used to detect the signals scattered from the clusters. However, the selection of a transducer depends not only on the signal amplitude for a given grain size and frequency, but also on the attenuation of the ultrasound in the tissue at that frequency. Such a trade-off makes 5 MHz a poor choice for this application. Our studies indicate however, that a 2.25 or 3.5 MHz transducer with appropriate gain compensation included in the scan system would be satisfactory.

Ultrasound travels in human breast tissue with a speed of 1500 to 1550m/sec. It is attenuated by various mechanisms, including scattering and absorption. The mechanism by which ultrasound is absorbed by biological materials is rather complicated. No general theory of absorption has been proposed. However, the measured absorption coefficient for soft tissue is approximately proportional to the frequency, f, and usually lies in the range 0.5 to 3.5

dB/cm-MHz (Wells 1977). A 50 dB attenuation in the sound intensity for a 10 cm distance is expected at 2.5 MHz, if d/f = 2 dB/cm-MHz. This 50 dB drop in signal amplitude would require a wide dynamic range for the signal detection system if no gain compensation were to be used.

We have conducted a series of experiments investigating how ultrasound scatters from small particles and used the results to design an ultrasound scheme which can uniquely identify these particles.

EXPERIMENTAL MEASUREMENTS

The prototype ultrasound equipment that we used for most of this work consisted of a pulsed emitter transducer operating at a mean frequency of 2.25 MHz which was also used as a receiver. The transducer was mounted so that it could easily be rotated through the arc of a circle in order to view the targets from different angles but in the same plane. The target was mounted on a movable platform whose position could be varied over a few centimeters in the x, y, and z directions. Such an arrangement allows a three dimensional scan of the cluster region to be made.

In order to distinguish ultrasound scattering from granular calcifications and from the tissue reflection, we used the criterion that the signal should be detectable at approximately equal intensity from more than one transducer position. This is possible since the scattering of sound by particles whose mean diameter is comparable to the wavelength of sound extends over a 2π scattering angle and, in general, has an appreciable intensity over the range of angles used here (Hueter and Bolt 1955). Since the scattered intensity for a given angle, ϑ, of the transducers is independent of azimuthal angle, transducers imaging the same plane at different angles should detect comparably sized signals, modified only by the different tissue absorption, depending on the particular path from

transducer to scatterer.

This approach is quite successful as can be seen from the scatter amplitude measurements shown in Figure 3. In this experiment, a 0.5 mm Cu wire and a 0.5 mm CaCO3 grain were mounted on a plastic slab 6 mm thick. Since the wire was attached to the slab by its ends, a few millimeters of space existed between the wire and the slab which was sufficient to resolve the wire signal from the slab signal when the slab was perpendicular to the beam. Measurements were made on the wire and then the slab was moved in order to bring the grain into the beam. The measurements show that at both 2.25 and 3.5 MHz the signal from the slab had decreased to zero when the angle of incidence was greater than 10 degrees from the perpendicular. In both cases the wire signal was nearly constant and identical at both frequencies. This would be expected since the wire diameter was chosen in the range where Figure 2 shows that we would expect a constant signal. Similar results were also obtained from the grains, although the average scattered signal was considerably smaller than that from the wire as expected since the grain presents a much smaller cross-section for scattering than does the wire. These results show that there is no problem distinguishing grain signals from large specular reflecting boundaries, if the scan angle is randomly selected and avoids the reflection angle. Hence, to ensure that the received signal is from a scatter source and not a large specular reflecting surface, it is necessary to aim the transducer from several different angles and then correlate the results. A tissue interface oriented at the appropriate angle for specular reflection to any one of the transducers can occur; in that case, only one transducer will detect a large signal. However a scatter source, such as calcifications, would be detected by all transducers.

Calcium carbonate grains of various diameters and cluster sizes were embedded in gelatin-Solkafloc (Picker Corp.) phantoms, in samples of human

breast tissue, and in beef liver. In Figure 4 we show the signals from a ten grain cluster (grain diameter 0.2 to 0.4 mm) in a gelatin-Solkafloc phantom using transducer frequencies of 5 and 2.25 MHz. In Figure 5 we show the signal from calcium carbonate grains embedded in breast tissue (A) and in beef liver (B), using 2.25 MHz transducers. As can be seen from the figures, the background scatter from the breast tissue and the liver medium is only slightly higher than that of the gelatin-Solkafloc phantoms and is still appreciably smaller than the scattered signal from the grain clusters.

A prototype B-scan configuration (Figure 6), with no compensation for signal attenuation, was used to produce the tomogram in Figure 7b. Figure 7a shows an x-ray photograph of the same phantom. The gelatin-Solkafloc phantom had an elongated cluster of 24 grains of 0.5-1 mm diameter embedded in it. The B-scan tomogram was created by using the x, y, z positioning screws shown in Figure 6 to move the sample through the median plane. The tomographic display was produced on a Tektronix 4012 graphic display terminal. In a clinical situation, of course, the transducer array would be automatically moved mechanically or steered electronically to provide full tomographic coverage of the breast region in a series of parallel planes, with different viewing directions in each plane.

It should be noted that the number of dots in the B-scan displays need not equal the number of scattering grains for the following reasons: (a) although the Picker and Aerotech tranducers that we used were damped, their response to a single grain was still three or four damped oscillations; (b) depending on the nearest neighbors distance distribution between the grains in the clusters, interference effects can occur which change the amplitude of some oscillations; (c) more dots can result if the cluster is over-scanned by recording receive signals from the cluster for transducer positions closer than the width of the

incident beam at the cluster position. Factors (a) and (c) can be programmed a priori into the computer display and a correction for (b) can be made after the initial scan.

The linear amplifiers, timing discriminators, and other recording electronics that we used were optimized for this stage of the project in order to search for calcification clusters of known size and position within the phantom. However we were curious to see whether the conventional diagnostic ultrasound machines were capable of mapping out the clusters in our phantoms. For this purpose we used a Rohe Compound B-scanner and a Varian electronically steered heart scanner with our samples. The results of scanning a cluster of 10 grains (grain diameter = 0.2 to 0.4 mm) are shown in Figure 8. The gain controls and other features had to be set precisely in order to see the grain clusters without flooding the scan with extraneous reflections. Furthermore, neither of these machines has provisions for systematic volume scans and signal correlations; hence, it is unlikely that such clusters could be detected reliably by conventional means in clinical situations, without a priori knowledge of their existence.

Tissue interface reflections were simulated by scanning a phantom that consisted of a cluster of 20 grains (0.4 to 0.6 mm in diameter) distributed in a circular area of $\approx$ 1 cm^2 and a specular interface made from a strip of flannel backed vinyl. The scanning arrangement and two tomograms (pixel size = 3 × 3 mm) are shown in Figure 9. In the zero degree tomogram the container walls are clearly shown. Both tomograms show the cluster location and the interface location. However, it is important to note that the cluster location is well-defined in both, and that different segments of the interface appear at different locations in the two photographs. The display format and the mechanical scanning arrangement for the correlation B scans is shown in Figure 9a. Note that

the transducer can be moved through an angle to either side of the zero degree position. For mechanical reasons involving the mounting of the phantom, the direction of rotation of the tranducer was to the left of the zero degree position.

MEASUREMENTS WITH AUTOMATIC GAIN AMPLIFICATION

In order to improve the technique and confirm that computer correlations of scans from different directions could indeed locate uniquely calcification clusters, one basic problem needed to be solved. This was to design an amplification system that compensated automatically for the tissue attenuation encountered along the path length. Such a system must be able to compensate for the differences in tissue attenuation that may vary from patient to patient in a clinical situation without intervention from the attending technician. Initially the computer would determine background signal level and set the gain control. The average level of background signals would then be stored for future subtraction from the measured amplitudes of the signals during the actual scan. The initial tomograms would then be basically free from ordinary tissue scatter, with specularly reflecting boundaries and cluster grain signals visible in the tomograms. To first order this is correct. However, some additional background subtraction may be necessary when fatty globules are present in the scan path.

This correlation technique was tested on a number of phantoms. As shown below the basic correlation method works well in locating the clusters uniquely. The main problem was that the size of the correlated cluster sometimes appears reduced in size. That is, the condition requiring comparably sized signals in each pixel tends to eliminate pixels that are on the edges of the cluster. In some cases the areas of the clusters were reduced by as much as a factor of 1.5.

Figure 10 shows a block diagram of the scan electronics that we developed to solve these problems. Signals sent simultaneously from the computer pulse

to the transducer, set the gain adjustment on the exponential amplifier and gated the integrator. By sampling the background signals with no compensation in the system, a least squares fit is made to determine the absorption coefficient α. This value of α then becomes the exponent used by the exponential gain amplifier to provide the compensatory gain. The computer then sets the amplifier system to the appropriate gain and samples the background once more. The fitting process is repeated until the proper compensation is established. The size of the compensated background signal is then measured and stored for future use. The resulting scan system was then used to scan Solka-floc phantoms. Figure 11 shows the results of scanning a phantom that consisted of a gelatin-Solka-floc mixture (5% Solka-floc by weight) with a 1 cm size cluster of calcium carbonate grains (0.4 to 0.6 mm grain size) embedded in it. In addition, a curved specularly reflecting boundary made from polyethylene was inserted near the cluster. A schematic of this phantom is shown in Figure 13c. A wire mesh was secured to the outside of the plastic container in order to provide a trigger signal to the electronics at the phantom boundary.

Scans of the phantom were taken at four angles from 0 to 30 degrees at 10 degree intervals. As can be seen in Figure 9a, signals due to the cluster, boundary and wire mesh are visible in all four tomograms. Portions of the wire mesh are seen at all angles for reasons described earlier. Different segments of the plastic boundary are also seen in the different views depending on the angle of the scan. The computer then subtracted the measured background level from each tomogram and then correlated the tomograms. It was asked to keep only those pixels for which all four tomograms showed comparably sized signals. All other pixels were set to zero. The resulting correlation tomogram is shown in Figure 11b. As can be seen only the cluster and a portion of the wire mesh satisfy the correlation condition. The resulting cluster is about 2 pixels on a

side; edge pixels were eliminated by the correlation condition.

To simulate the effect of fat globules in tissue, we constructed a phantom with a cluster of 20 grains (grain diameter = 0.4 to 0.6 mm; cluster diameter = 1 cm) in a gelatin-Solkafloc mixture, and injected a large globule of vegetable oil. Figure 12 shows a comparison of the amplitudes of the signals received from an oil globule and the cluster; in general, the grain signals are at least a factor of 2 larger. Figure 13 shows the correlation tomograms of this phantom. At high sensitivity both the cluster and the oil meet the correlation condition of comparably sized signals in all four angle scans. By manually inputting a higher background level (reducing the sensitivity), only the cluster meets the correlation conditions. Thus, such a scanning system should be able to distinguish fatty globules from calcification clusters by preprogramming the display system for a sensitivity appropriate for the clusters to meet the correlation condition, for calcifications but not fat.

CONCLUSIONS

Using an ultrasound scan system operating at 2.25 MHz and with automatic gain compensation, we have shown that it is possible to detect the scattered signals from clusters of calcium carbonate grains embedded in phantoms consisting of plastic containers filled with gelatin-Solkafloc media. Measurements on breast tissue samples in which calcium carbonate grain clusters were embedded show that the interfering scattered signals from normal tissue are appreciably smaller than grain cluster signals, and hence can be distinguished electronically. In normal and abnormal breasts there can be large tissue interface specular signals. The scatter signals can be discriminated against by setting up a correlation function in the computer that compares tomograms of the same plane obtained at different angles and selects only those pixels in which there

are comparably sized signals in all the tomograms. The assumption we make is that a tissue interface or other structure capable of reflecting a large specular signal is unlikely to reflect it back onto more than one receiver at any given measuring position. In addition it is possible to distinguish cluster correlations from those obtained from fatty globules in the tissue by reducing the sensitivity of the scan. Since the oil globule signals are appreciably smaller than the grain signals, they will not correlate at a reduced sensitivity.

REFERENCES

S.A. Feig, G.S. Shaber, A. Patchefsky, G.F. Schwartz, J. Edeiken, H.I. Libshitz, R. Nerlinger, R.F. Curley, J.D. Wallace (1977), "Analysis of clinically occult and mammographically occult breast tumors", Am. J. Roentgenology **128**, p. 403-408.

T.F. Hueter and R.H. Bolt (1955), SONICS, John Wiley and Sons, NY p. 83-85.

I.J. Malone, G. Frankl, R.A. Dorazio, J.H. Winkley (1975), "Occult breast carcinomas detected by xeroradiography: clinical considerations", Ann Surg **181**, p. 133-136.

W.A. Murphy, and K. DeSchryver-Kecskemti (1978), "Isolated clusted microcalcifications in the breast: radiologicpathologic correlation", Radiology **127**, p. 335-341.

V. Perez-Mendez, D. Ortendahl, G. Sommer, J. Baker, P. Wiedenbeck (1979), "Tomographic visualization of breast calcifications by ultrasound", IEEE TRANS. NUC. SCI. **NS 26**, p. 2826-2835.

E. Sickles (in press), "Tomographic detectability of breast calcifications".

Picker Corp. Solkafloc is an additive developed by this company to simulate liver and breast tissue in gelatin media. Made by Brown Co., Berlin-Gorham Division, Berlin, NH 03570.

P.N.T. Wells (1977), BIOMEDICAL ULTRASONICS, Academic Press, NY.

J.N. Wolfe (1974), "Analysis of 462 breast carcinomas", Am. J. Roentgenology **121**, p. 846-853.

FIGURE CAPTIONS

Fig. 1. X-ray picture of calcifications in breast tissue taken with fine focus x-ray tube.

Fig. 2. Scatter amplitudes from grains embedded in gelatin. Calculated and measured response for 2.25, 3.5, and 5.0 MHz transducers is shown.

Fig. 3. Scatter amplitudes from 0.1 mm wire Calcium Carbonate grain and a lucite slab 6 mm thick.

Fig. 4. Oscilloscope signals of scatter signal from Calcium Carbonate grains embedded in Gelatin-Solkafloc phantom. Transducer frequencies (a) 5 MHz and (b) 2.25 MHz.

Fig. 5. Oscilloscope signals of Calcium Carbonate grains embedded in breast tissue (a) and in beef liver (b). Transducer frequency 2.25 MHz.

Fig. 6. Experimental arrangement of (a) Transducer positioner and sample in water bath and (b) Prototype scanning configuration.

Fig. 7. (a) X-ray picture (fine focus tube) of Calcium Carbonate grains (0-5 to 1.0 mm diameter) embedded in Gelatin-Solkafloc phantom and (b) Ultrasound B-scan of same cluster.

Fig. 8. Ultrasound scans of 10 grain cluster (0.2-0.4 mm diameter) in Gelatin-Solkafloc taken with (a) Rohe Compound B scanner and (b) Varian heart scanner.

Fig. 9. Ultrasound tomogram of grain cluster and curved plastic layer embedded in gelatin phantom. (a) Transducer arrangement and (b) Computer display of grains and plastic interface.

Fig. 10. Block diagram of automatic gain compensation electronics.

Fig. 11. Tomograms of grain cluster, boundary mesh, and interface plastic layer. (a) Scans taken at four different angles, (b) Correlation scan display, and (c) Schematic of phantom.

Fig. 12. Analogue display of scatter signals taken at 2.25 MHz. (a) Calcification and (b) Oil globule.

Fig. 13. Correlation tomogram of oil globule and calcification cluster at (a) High sensitivity and (b) Low sensitivity.

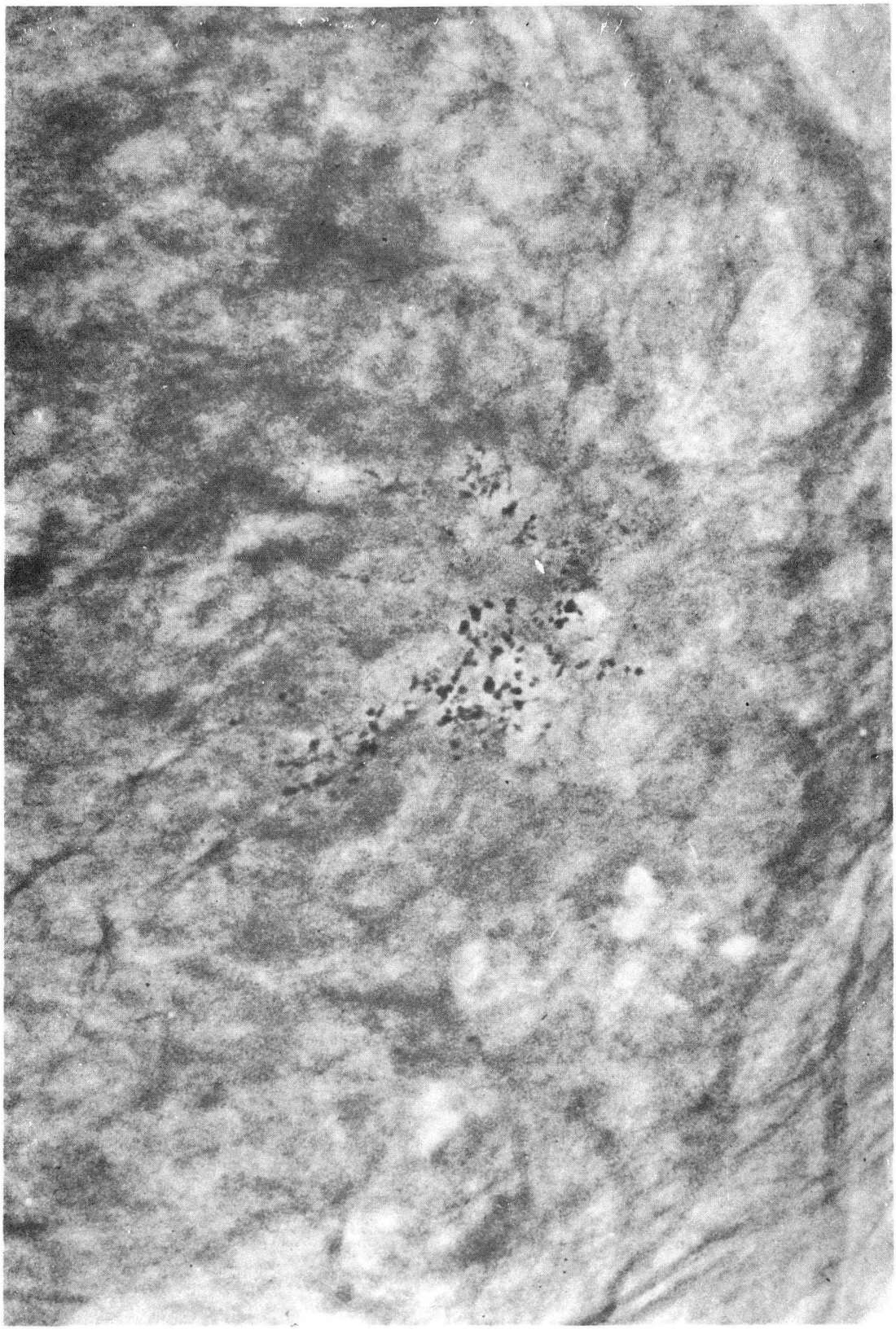

Fig. 1

XBB 792-2230

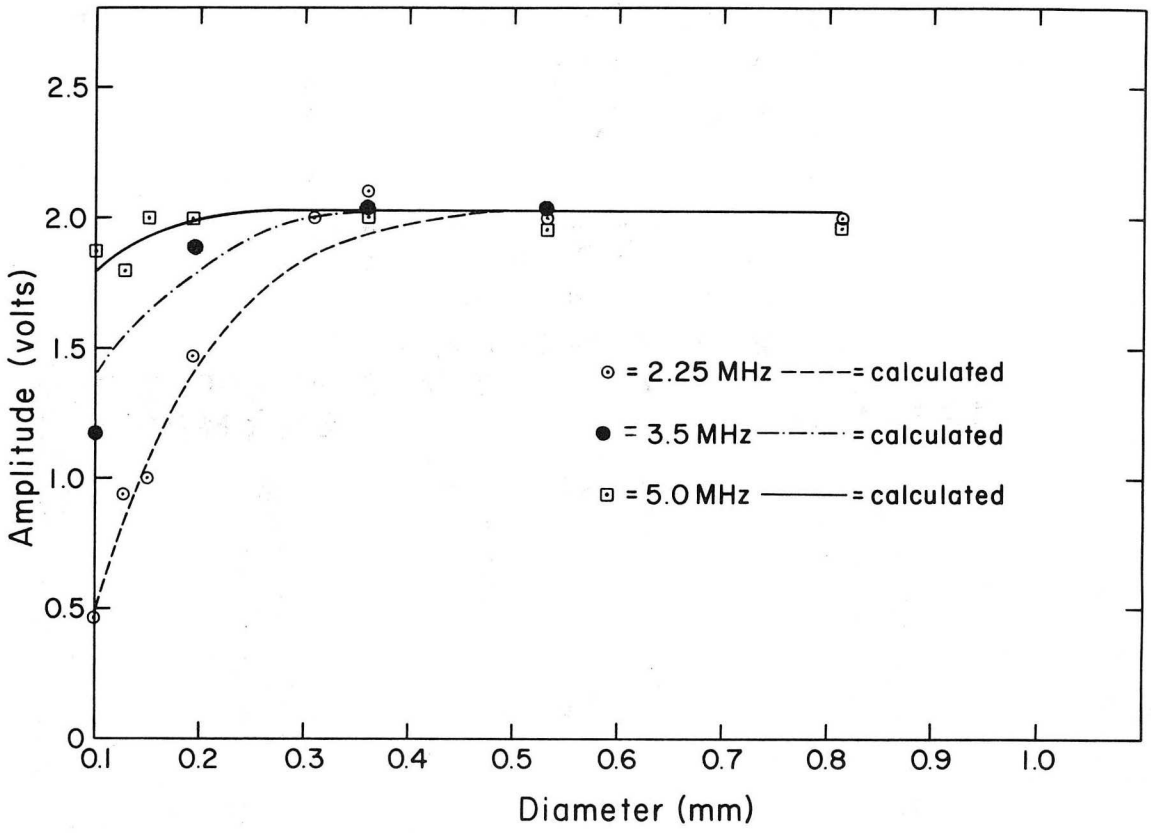

XBL 7812-13755A

Fig. 2

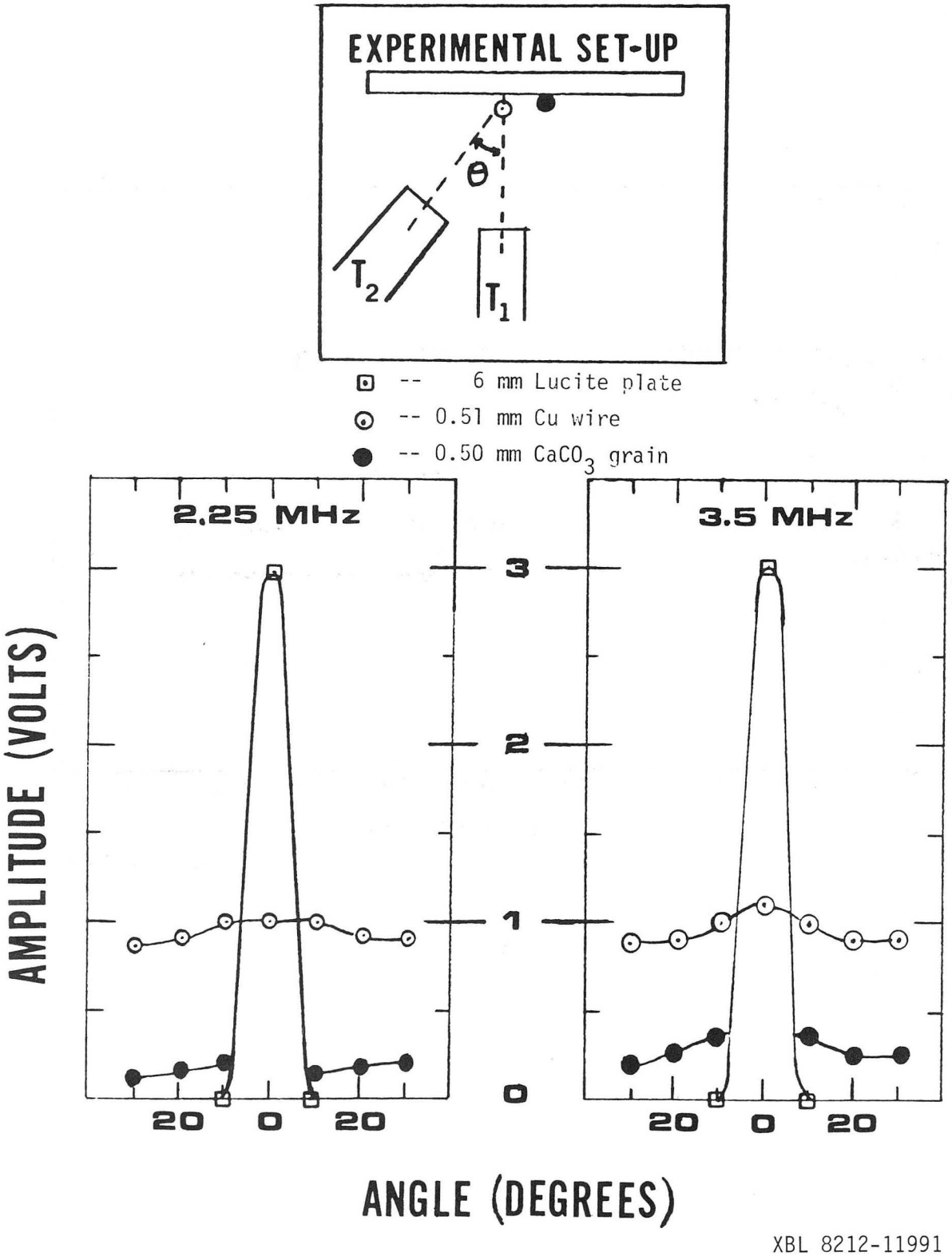

XBL 8212-11991

Fig. 3

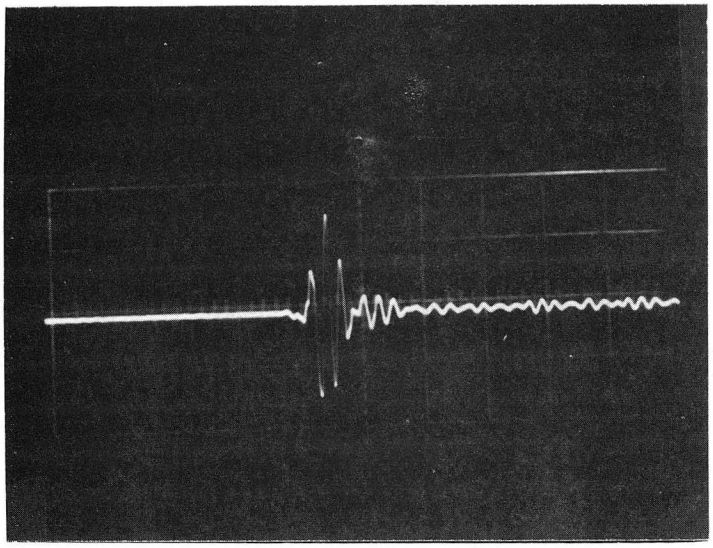

A

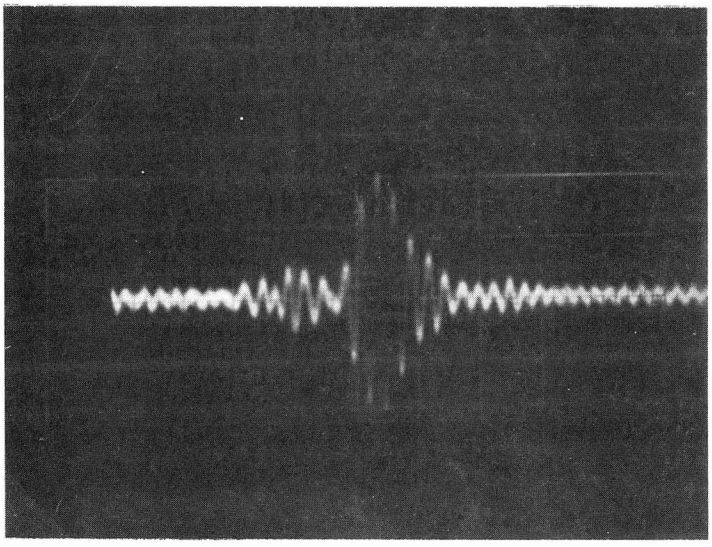

B

XBB 780-15458

Fig. 4

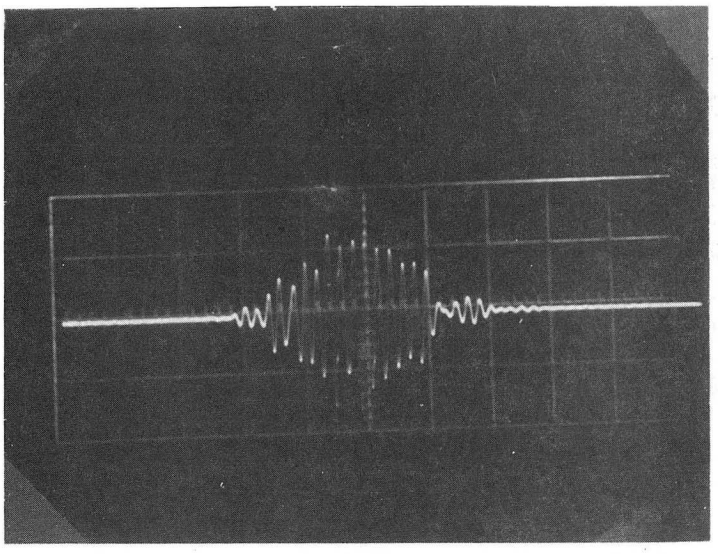

A

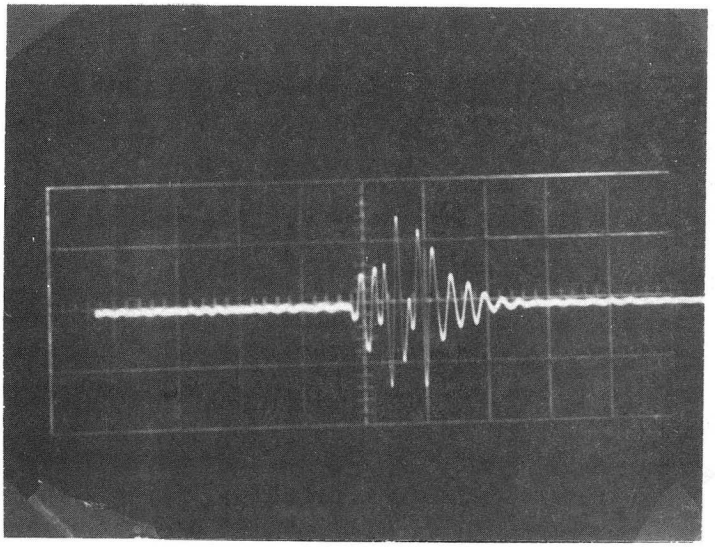

B

XBB 780-15459

Fig. 5

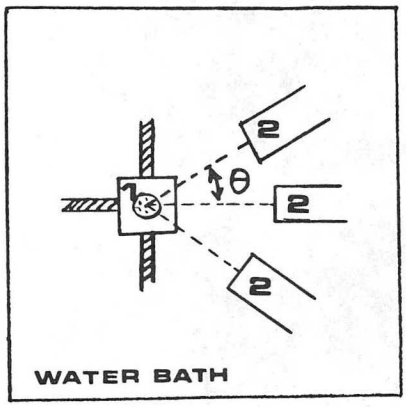

1 PHANTOM
2 POSITIONS OF TRANSMIT-RECEIVE TRANSDUCER

EXPERIMENTAL CONFIGURATION

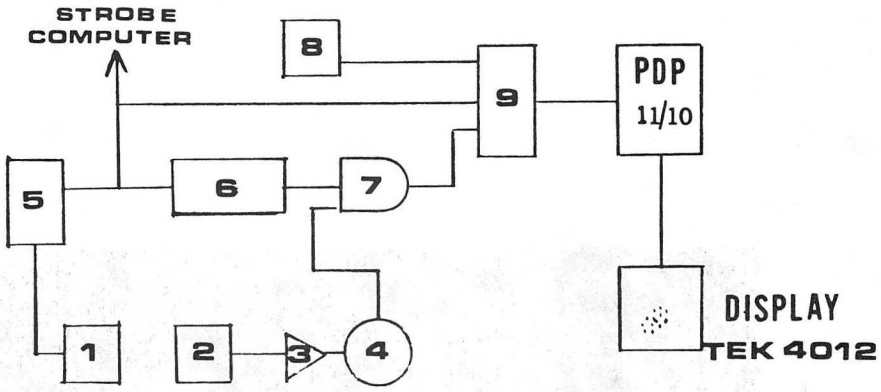

1 TRANSMITTER
2 RECEIVER
3 AMPLIFIER
4 DISCRIMINATOR
5 HV PULSER
6 DELAYED GATE GENERATOR
7 AND GATE
8 10 MHZ CLOCK
9 SCALER

PROTOTYPE SCANNING CONFIGURATION

XBL 8212-11992

Fig. 6

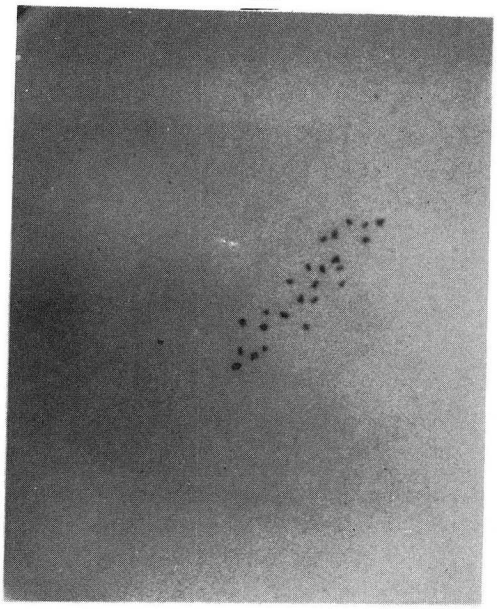

A

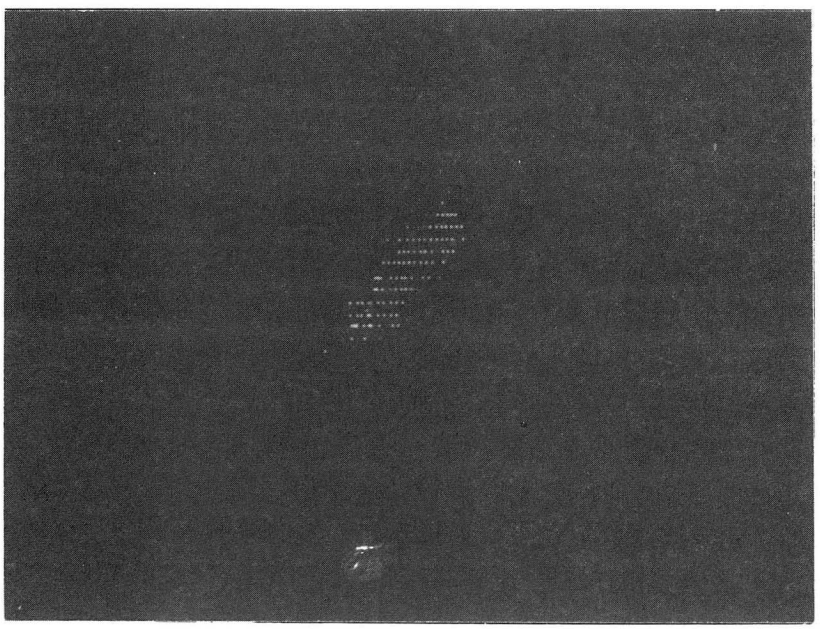

B

XBB 780-15460A

Fig. 7

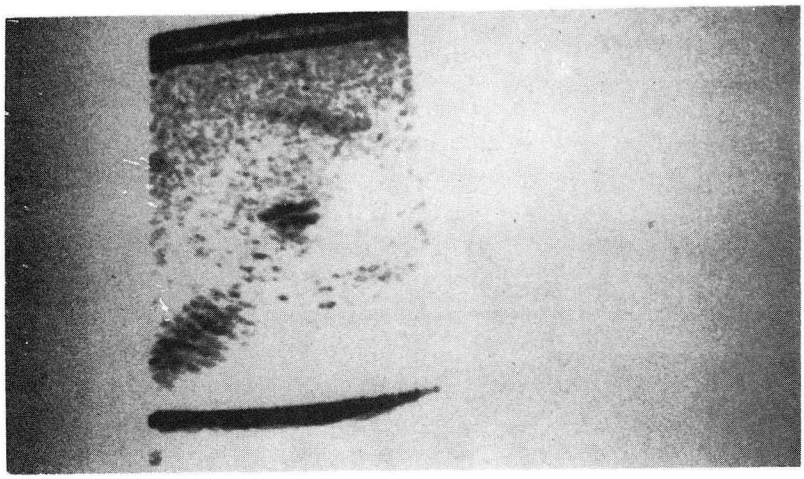

(a) B-scan. Rohe machine.

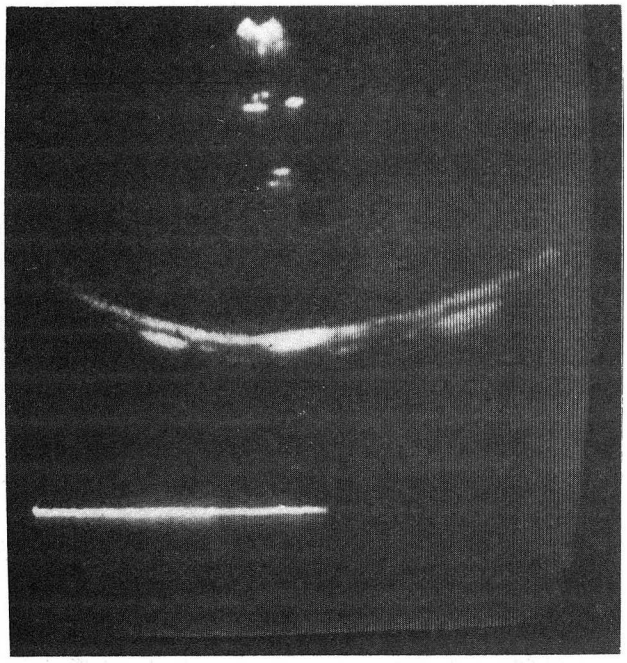

(b) B-scan. Varian cardiac machine.

Scans of calcification clusters.
Ten grains each (0.2-0.4 mm dia.)
in gelatin-Solkafloc medium.

XBB 780-15411

Fig.8

1 MICROCALCIFICATIONS
2 TRANSDUCER POSITION

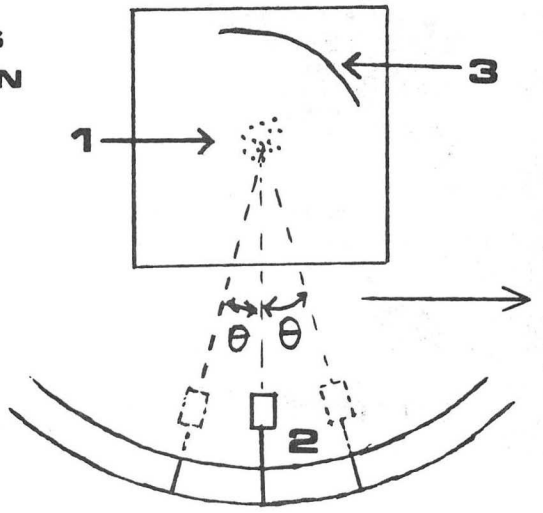

DIRECTION OF
PHANTOM MOTION

TOMOGRAMS AT TWO ANGLES

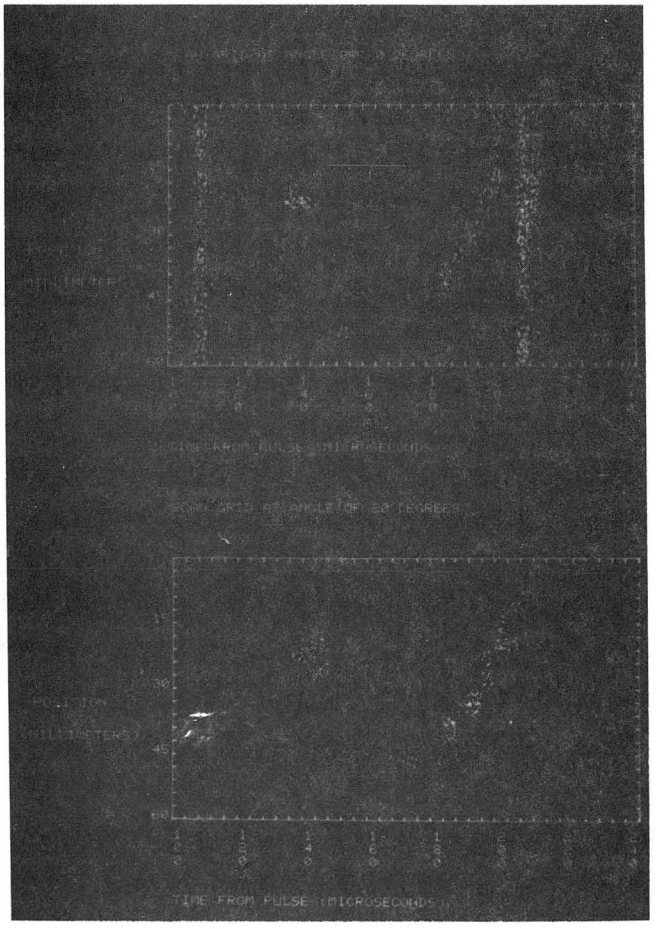

XBB 820-10260

Fig. 9

ELECTRONIC BLOCK DIAGRAM

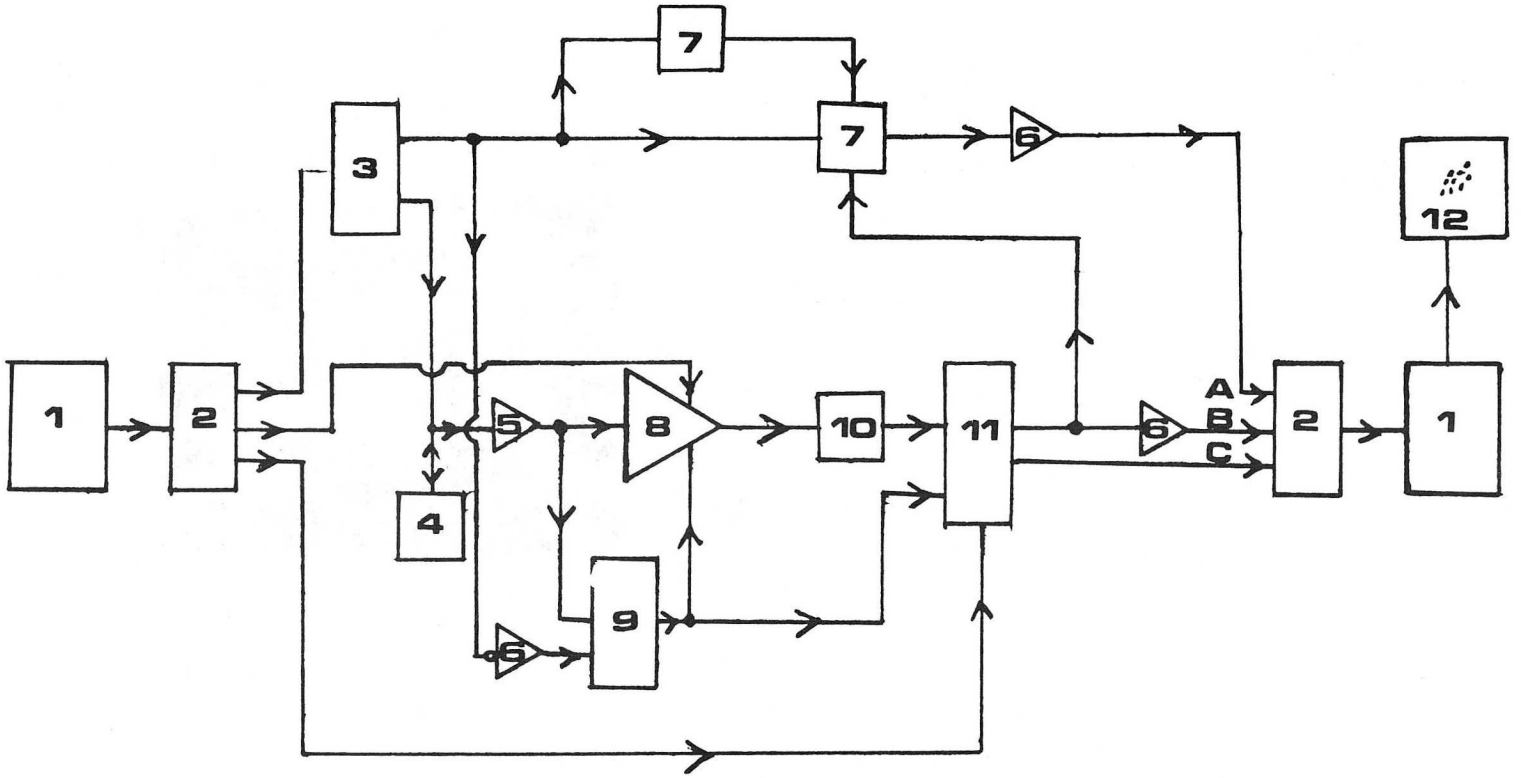

1 PDP 11/10
2 CAMAC
3 HIGH VOLTAGE PULSER
4 TRANSDUCER
5 PREAMPLIFIER
6 LEVEL SHIFTERS
7 GATE GENERATOR
8 EXPONENTIAL AMPLIFIER
9 FIRST ECHO TRIGGER
10 RECTIFIER
11 INTEGRATOR
12 TEKTRONIX 4012

A SCALER INHIBIT
B ADC GATE
C ANALOGUE OUT

XBL 837-10818

Fig. 10

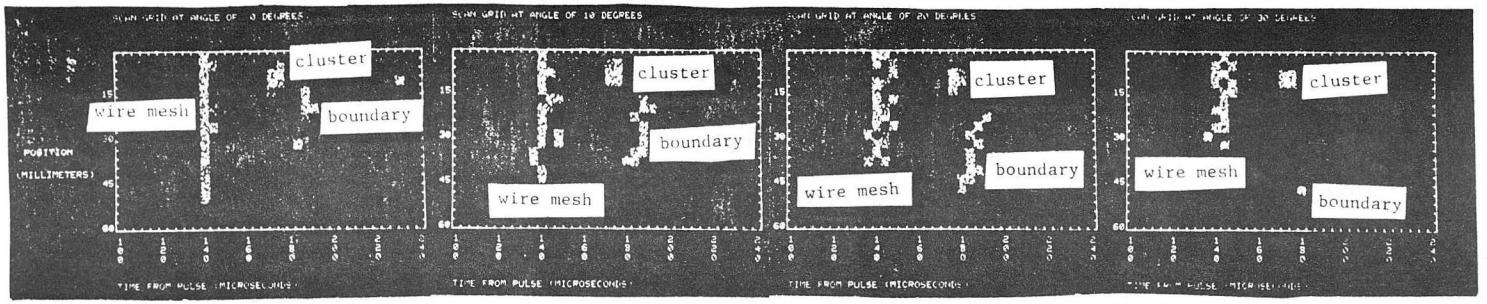

TOMOGRAMS AT FOUR ANGLES

A

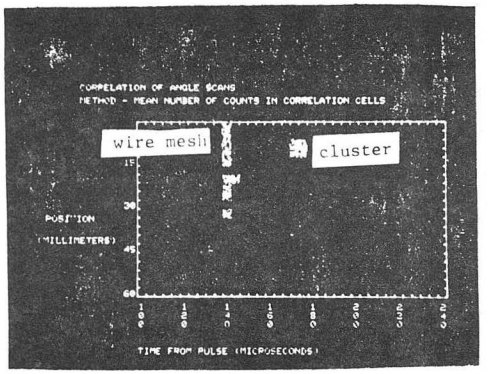

CORRELATION TOMOGRAM

B

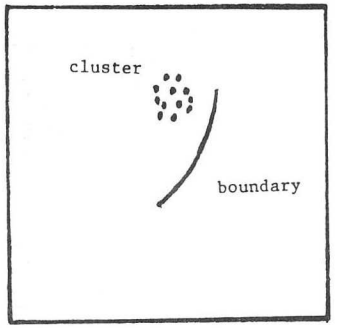

PHANTOM SCHEMATIC

C

PHANTOM DESCRIPTION

The cluster consists of
20 calcium carbonate grains.

GRAIN DIAMETER -- 0.4 - 0.6 mm

CLUSTER DIAMETER -- 1 cm

XBL 837-10817

Fig. 11

ANALOGUE SIGNALS AT 2.25 MHz

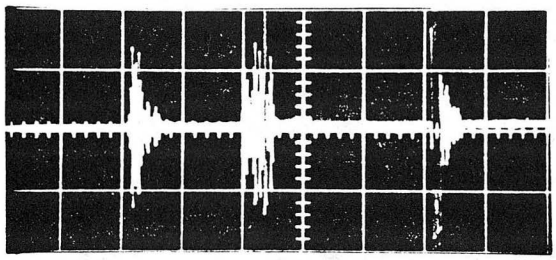

CLUSTER SIGNAL

Horizontal -- 1 Volt/cm

Vertical -- 20 μsec/cm

A

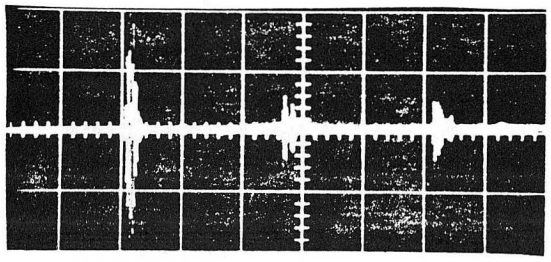

OIL SIGNAL

Horizontal -- 1 Volt/cm

Vertical -- 20 μsec/cm

B

In both instances, the end sets of oscillations are due to the walls of the container.

XBL 837-10815

Fig. 12

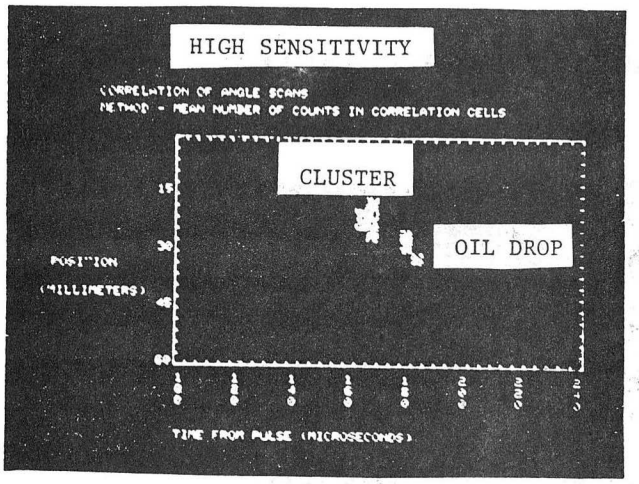

A

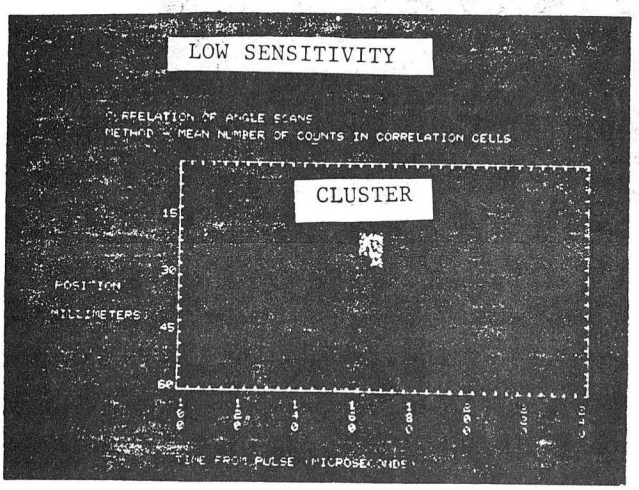

B

XBL 837-10816

Fig. 13

TECHNICAL INFORMATION DEPARTMENT
LAWRENCE BERKELEY LABORATORY
UNIVERSITY OF CALIFORNIA
BERKELEY, CALIFORNIA 94720